ELSEVIER

Journal of Nuclear Materials 294 (2001) 305–314

journal of nuclear materials

www.elsevier.nl/locate/jnucmat

Study of surface modification of uranium and UFe_2 by various surface analysis techniques

O. Bonino [a], O. Dugne [a], C. Merlet [b,*], E. Gat [c], Ph. Holliger [d], M. Lahaye [e]

[a] *CEA VALRHO–DCC/DTE/SIM, Laboratoire de Métallographie, BP 111, Pierrelatte 26702, France*
[b] *CNRS-ISTEEM, Université de Montpellier II, Pl E. Bataillon, Montpellier 34000, France*
[c] *BIOPHY Research S.A., 6 Rue Anne Gacon, Marseille 13016, France*
[d] *CEA GRENOBLE–DTA/LETI/SCPM, Grenoble 38054, France*
[e] *CNRS-CECAMA–ICMCB, Pessac cedex 33608, France*

Received 19 June 2000; accepted 5 January 2001

Abstract

The surface modification of U, UFe_2 by exposition in air at room temperature and at 63°C was studied by secondary ion mass spectroscopy (SIMS), time of flight-secondary ion mass spectroscopy (ToF-SIMS), Auger electron spectroscopy (AES) and X-ray photoelectron spectroscopy (XPS) with variable detection angle. For the two systems, a first layer of carbon contamination, followed by complex oxide layer constitutes the surface. For U, the oxide layer is composed of a mixture of UO_2 and UO_{2+x} with x maximal at the surface. In UFe_2, the oxide layer is composed of a mixture of UO_2 and UO_{2+x}, oxidised iron in Fe2+ and Fe3+ chemical states (more probably FeO), a few percent of a ternary oxide $UFeO_4$, and less than 1% of uranium carbide. A surface segregation of uranium is shown in UFe_2.

PACS: 68.35.B; 82.80.−d; 81.65.Mq; 74.70.A

1. Introduction

The knowledge of the surface of the uranium-materials is necessary to the reliability of the analysis of those materials by wavelength dispersive spectroscopy electron probe microbeam (WDS-EPMA). It is well known that WDS-EPMA is a powerful technique to quantify the local elementary concentration of phases presented in the material. Its principle proposed by R. Castaing in 1951 is based on the excitation of the matter by an electron beam which generates an X-ray signal characteristic of the present elements. This technique has been used very early in the nuclear laboratories especially to detect and quantify the fission products of the worn fuels. However, to have accurate results, the measurement by WDS-EPMA needs a perfect flat polished surface, but, unfortunately after a metallographic preparation, those compounds become oxidised immediately. An oxide layer covers the surface [1–7], and the surface modification (contamination, oxidation) modifies and contributes to the quantitative analysis results obtained by WDS-EPMA. As a result, the X-ray measured signal is non-representative of the bulk and induces analysis errors. These errors due to the contribution of the surface are present not only in WDS-EPMA but also more generally in all analysed techniques based on X-ray spectrometry. Nevertheless, a good knowledge of the surface structure associated with a multilayer software for WDS-EPMA allows to improve the accuracy of the bulk concentration by removing the surface contribution [8]. Furthermore, this contribution constitutes a progress in the knowledge of the interfacial surface chemistry in the initial stages of oxidation of such materials.

With a view to improve the accuracy of X-ray spectroscopy, this work is devoted to study the surface of uranium-materials (uranium, UFe_2) after

* Corresponding author. Tel.: +33-4 67 54 42 17; fax: +33-4 67 14 47 85.
E-mail address: merlet@dstu.univ-montp2.fr (C. Merlet).

0022-3115/01/$ - see front matter
PII: S0022-3115(01)00432-9

metallographic preparation. Secondary ion mass spectroscopy (SIMS), time of flight-secondary ion mass spectroscopy (ToF-SIMS), Auger electron spectroscopy (AES) and X-ray photoelectron spectroscopy (XPS) with variable detection angle are jointly used. These techniques are complementary. AES is used to measure the elementary concentration. SIMS gives information about fluctuations of composition into a layer and permits to dissociate the layers of different physical–chemical nature. ToF-SIMS allows the physical–chemical nature to be studied. XPS with variable angle is used to study the elementary concentrations, their depth distribution and the physical–chemical nature. In AES, SIMS and ToF-SIMS ion abrasion has been used, the analysed depth is about several hundreds nm while by XPS the analysed depth is only about 7 nm.

2. Experimentation

Polycrystalline samples of uranium and UFe_2 were obtained by direct melting, afterwards the oxidation was operated in air at two different temperatures: room (20°C) and 63°C. At room temperature, the oxidation times were 4 and 10 h (the transport time to measurement installation) and at 63°C, the oxidation times were 45, 72 h and 17 days. Oxidation times at room temperature have been chosen to reproduce the surface in the measured conditions of WDS-EPMA. The oxidation occurring in the various installations of analysis techniques under primary or secondary vacuum was neglected.

Prior to all surface analyses, the sample surface is carefully cleaned. The sample preparation corresponds to one required in WDS-EPMA. The preparation is a mechanical polishing and the final polishing is achieved successively by polishing on a Struers OP Chem with OPU-colloidal silica of 0.04 μm in diameter. To finish, a rinse with non-ionised water, a rubbing on a dry tex and a drying for a few seconds with a compressed air throw; this last step contributes to produce chemisorbed water at the surface.

The X-ray photoelectron measurements were done with a Scienta ESCA 200 (Biophy Research S.A.) with variable detection angle and an ESCALAB 200 with a detection normal to the surface (CEA Saclay – SPCP). The X-ray source is the monochromatised AlK_α radiation (500 W) of energy 1486.6 eV. The analysed surfaces are, respectively, 1×1 mm^2 for the Escalab 200 and 0.4×2 mm^2 for Scienta ESCA 200 at normal detection angle. The four detection angles are 0° (detection normal to the surface), 60°, 70°, 75°. If the surface is assumed to be UO_2, the analysed thickness is respectively 8.4, −4.2, −2.9 and 2.2 nm for $U4f_{7/2}$ and 6.3, −3.15, −2.15 and 1.65 nm for $Fe2p_{3/2}$. These values are estimated from a relationship proposed by Seah and Dench [9]; the effective escape depth of the photoelectrons is approximately 2.8 nm. The typical relative error on concentration is 10–20%. The chemical analyses have been obtained by decomposition of C1s, O1s, $U4f_{7/2}$ and $Fe2p_{3/2}$ peaks.

The secondary ion mass measurements were done with a Cameca IMS5f (CEA DTA/LETI/SCPM). The primary emission is C_s^+ with an analysed surface of 250×250 μm^2 and the measured negative secondary ions are ^{16}O, $^{16}O^1H$, $^{56}Fe^{16}O$, $^{238}U^{16}O$, $^{238}U^{12}C_2$, $^{238}U^{16}O_2$. As the impact energy is 2 keV (C_s^+ 5 kV, secondary ions 3 kV), the thickness of mixing is about 2 nm. Finally, the crater depth after analysis has been measured with a profilemeter with a typical relative precision of 10%.

The Auger electron measurements were done with a VG Microlab 310F (CNRS–Cecama–ICMCB). The accelerating voltage of electrons is 10 kV, with a beam intensity of 3 nA. The energy resolution is 0.5%. Concentrations of U (U MN2-2756 eV), Fe (LM4-648 eV), O (KL1-506 eV) and C (KL1-272 eV) with typical relative precision of 20% are obtained with AES. For the argon ion bombardment, the accelerating voltage is 4 kV with a beam intensity of 250 nA. With these experimental conditions, the thickness of mixing is about several nm. The thickness and the surface of the analysed volume are respectively 3 nm and 50 μm^2.

The time of flight-secondary ion mass measurements were done with a Perkin Elmer Phi 7200 (Biophy Research S.A.). The accelerating voltage of the primary ion source of Cs^+ is 8 kV. The abrasion intensity is 75 nA dc, with an abrasion step of 2 s, and a death time of neutralisation of 10 s. The analysed surface is 10×10 μm^2. Some fragments of sample are sputtered and recombined. This technique allows very heavy ions (theoretically unlimited) to be detected.

3. Results and discussions

3.1. Uranium

The SIMS, AES and XPS analyses show that the surface of uranium oxidised in air at room temperature for 4 and 10 h and at 63°C for 72 h are constituted of two layers covering the uranium substrate (Fig. 1). Each of these layers has the same physical–chemical nature in uranium oxidised at room temperature and at 63°C, but with reduced thicknesses at room temperature.

The first layer is constituted of contamination carbon with a thickness of about 1–2 nm. This layer is detected by both XPS, AES and SIMS on uranium oxidised at room temperature and at 63°C. Indeed, 25% of carbon are measured by XPS with a detection normal to the surface on uranium oxidised at 63°C for 72 h (analysis

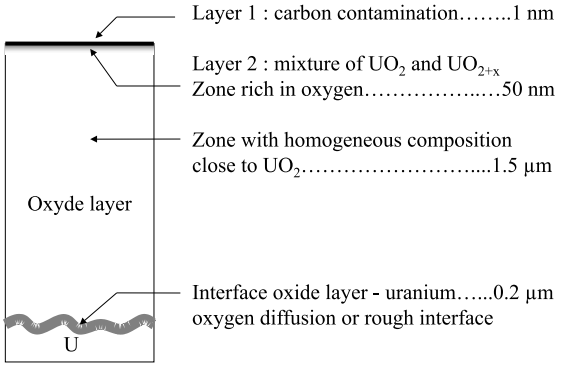

Fig. 1. Diagram of the uranium surface oxidised at 63°C for 72 h.

depth about 8 nm). Moreover, the AES concentration of carbon is the highest (more than 50 at.%) in the first nm of uranium samples oxidised at room temperature for 10 h (Fig. 2(a)). These XPS and AES results are characteristic of a thin carbon layer with a thickness less than 2 nm. The measured concentrations of carbon (25% by XPS and 50% by AES) are less than 100% which is the concentration of a carbon layer because the analysis depths of these two analysis techniques (about 8 nm for XPS and about 3 nm for AES) are more important than the carbon layer thickness (1–2 nm) in the present experimental conditions. By SIMS, the strong variations of secondary ion intensity of $^{16}O^1H^-$, $^{18}O^-$, $^{56}Fe^{16}O^-$, $^{238}U^{16}O^-$, $^{238}U^{16}O_2^-$ in the first nm are characteristic of an interface which separates two layers of different physical–chemical nature (Fig. 3(a)): this first carbon layer and the following oxide layer.

The second layer is an oxide layer constituted by a mixture of UO_2 and UO_{2+x} with $0 < x < 0.25$. Indeed, for uranium oxidised at 63°C for 72 h, in XPS, the 4f levels of uranium are typical of two components UO_2 and UO_{2+x} (Fig. 4) [10]. In fact, the binding energies of $4f_{7/2}$ level of uranium in UO_2 and UO_{2+x} with $0 < x < 0.25$ are respectively 380 eV with satellite peak at 386.9 and 381.25 eV with two satellite peaks at 385.4 and 389 eV (Fig. 4) [10]. It must be specified that several hundreds of nm in depth were measured by AES and SIMS analyses while the XPS depth analysis is lower than 10 nm. As a result, the secondary ion intensities (SIMS) values of $^{16}O^-$, $^{16}O^1H^-$, $^{238}U^{16}O^-$, $^{238}U^{12}C_2^-$, $^{238}U^{16}O_2$ of oxidised uranium at 63°C for 72 h between about 5 and 8 nm (after the carbon layer and mixing effect) are characteristic of a mixture of UO_2 and UO_{2+x} as obtained by XPS. Both for uranium oxidised at room temperature and 63°C, in the second layer, each of the secondary ion intensities is of the same order as these which is characteristic of a mixture of UO_2 and UO_{2+x} as

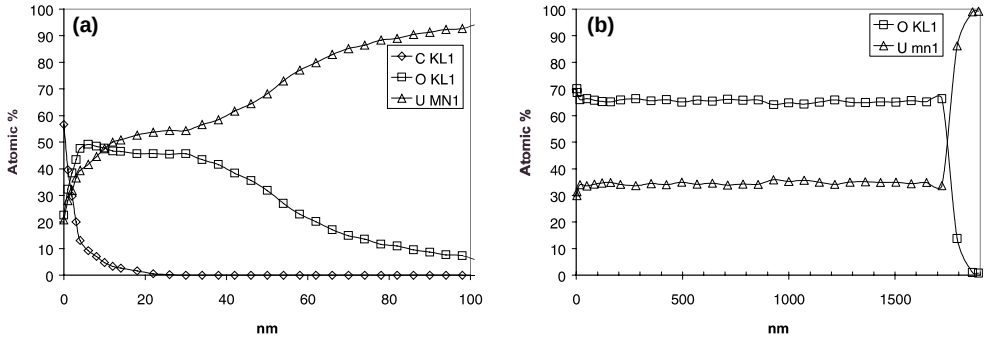

Fig. 2. AES profile of uranium oxidised: (a) at room temperature for 10 h; (b) at 63°C for 72 h.

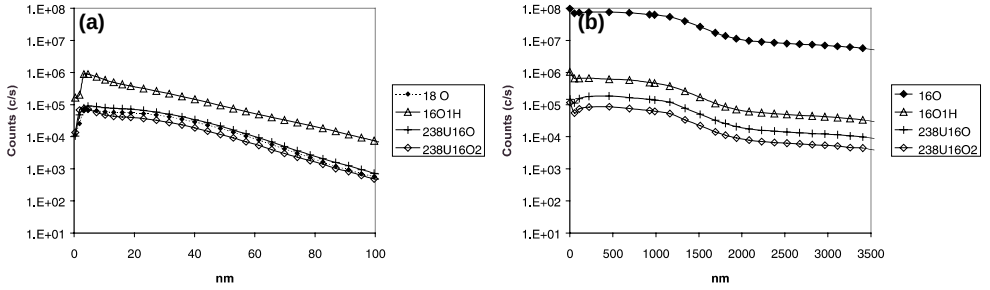

Fig. 3. SIMS profile of uranium oxidised: (a) at room temperature for 4 h; (b) at 63°C for 72 h.

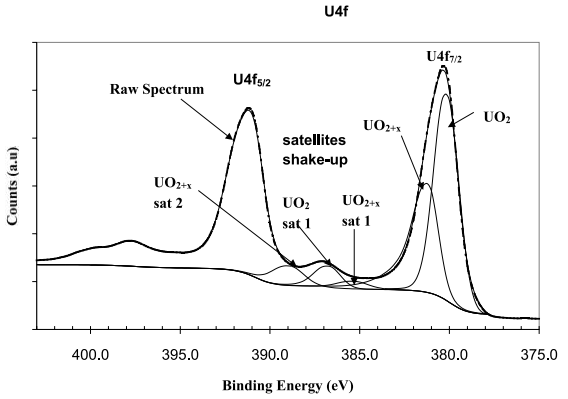

Fig. 4. XPS spectrum of U4f in uranium oxidised at 63°C for 72 h.

shown by XPS (from several nm to 20 nm on the Fig. 3(a), from several nm to 1 μm on Fig. 3(b)). As a result, the chemical–physical nature of these layers is a mixture of UO_2 and UO_{2+x}.

The second layer thicknessess are respectively from 10 to 20 nm (Fig. 3(a)) for uranium oxidised at room temperature for 4 h and 40 nm (Fig. 2(a)) for uranium oxidised at room temperature for 10 h. Its thickness is 1 μm by SIMS (Fig. 3(b)) and 1.8 μm by AES (Fig. 2(b)) for uranium oxidised at 63°C for 72 h. The AES and SIMS analyses have been done on two different regions of the surface. The differences of thickness values could be attributed to a heterogeneity of the oxide layer thickness or to the different techniques used to measure the thickness in AES and SIMS.

For uranium oxidised at room temperature, the AES oxygen concentration fluctuation could be interpreted as the following (Fig. 2(a)): The second layer constituted of a mixture of UO_2 and UO_{2+x} rich in oxygen in the first tenth nm. This layer contains some carbon. The AES concentration of carbon decreases in the first 20 nm. The carbon is located less deep than oxygen atoms in the sample.

For uranium oxidised at 63°C for 72 h, the composition is rich in oxygen (about $UO_{2.25}$) onto the near surface of this mixed layer of UO_2 and UO_{2+x}. O/U ratio decreases rapidly and the composition tends to UO_2 over the first 50 nm as it is proved by the decrease of the AES concentration of oxygen by 16% over the first 50 nm. (Fig. 2(b)). Further, the composition is homogeneous and close to UO_2 over its thickness. Indeed, the AES composition and the secondary ion intensities are constant (with 20% typical accuracy by AES) (Figs. 2(b) and 3(b)) and are consistent with a homogeneous composition close to UO_2 over the oxide layer thickness (Fig. 2(b)). The AES carbon concentration has not been measured; no conclusions can be done on carbon penetration at 63°C.

The oxide layer–uranium interface is characterised by the decrease of one order of magnitude of secondary ion intensities, and by the decrease to zero of AES oxygen concentration, from a few nm to 100 nm for uranium oxidised at room temperature for 4 and 10 h and from 200 to 600 nm for uranium oxidised at 63°C for 72 h (Figs. 2 and 3). This observed interface could be a region where oxygen diffuses in uranium and/or could be a consequence of a rough oxide layer–uranium interface (due to mixing induced by ion bombardment in AES and SIMS).

The initial oxidation of polycrystalline uranium of high purity by exposure to O_2 [6,11], CO [6], CO_2 [6], and water vapour [4] has been extensively studied. The absorption of these gases induces the creation of an oxide UO_{2+x}. The exposure to CO and CO_2 induces a complete dissociation of CO or CO_2 or a C–O bond. Oxygen is transported in uranium in the form of O_2^- or OH^-. The carbon is produced by the dissociation of CO and CO_2 which diffuses into the bulk of the metal and forms a carbide. Bulk oxidation mechanisms for reaction of dry O_2 with clean uranium are well understood [12]. O_2 is molecularly chemisorbed onto the clean uranium surface. It rapidly dissociates and combines with the surface uranium atoms to form an oxide layer. Once the initial oxide layer is formed, molecular oxygen continues to adsorb on the oxide surface. Most of it is transported into the oxide lattice in the form of O_2^-. Some oxygen remains on the surface as chemisorbed O_2^- or O^-, or in the near surface as interstitial O^-. An oxide UO_{2+x} in excess of the stoichiometric value of two is created. For a long exposure time the entire oxide layer becomes interstitial rich UO_{2+x}.

This study confirms that the oxide layer is a mixture of UO_2 and UO_{2+x} hyperstoichiometric onto the surface. The oxygen concentration decreases on the 50 nm and is constant deeper. The form in which the oxygen diffuses is non-determined by this study. The carbon atoms penetrate into uranium in the first 20 nm, less deep into the sample than the oxygen atoms do after 10 h of oxidation at room temperature.

Table 1 presents the different layers and their thickness measured by AES, SIMS and XPS with detection normal to the surface between the conditions of oxidation.

3.2. UFe_2

The surface of UFe_2 has been studied by XPS, SIMS, AES and ToF-SIMS.

The XPS with variable angle gives information about the elementary concentrations, the elementary depth distribution and the physical–chemical nature in the first 0–7 nm. By XPS with variable detection angle, only uranium, iron, oxygen and carbon are detected a few hours (4–10) after metallographic preparation of the

Table 1
Thickness of the different overlayers found in the surface on uranium

	Between 4 and 10 h at room temperature (nm)	72 h 63°C
Contamination carbon	⩽2	⩽2 nm
Mixture of UO_{2+x} and UO_2		
Zone rich in oxygen	0	0.05 μm
Zone with composition close to UO_2	≈7–40	1.05–1.95 μm
Metallic uranium	+	+

surface of UFe_2. If other elements are presents, they are just in trace (<1%). The XPS measured elementary concentrations (in at.%) are shown in the Table 2.

A strong variation of composition appears between normal and 60° detection angle: the proportion of carbon and the ratio U/Fe increase greatly near the surface. This trend decreases slowly for high tilted angle (70°). Between 70° and 75°, the compositions are very similar. For a normal angle (0°), the Fe/U ratio is about 1. For grazing angles, the uranium concentration is stable at about 7.5% while the iron concentration decreases to 2% on the near surface. The first or two first nm are constituted of an outermost layer of contamination carbon, followed by an oxide layer with an iron depletion over more than 7 nm. At a depth of 7 nm, iron and uranium concentrations are similar.

The chemical analysis results obtained by decomposition of C1s and O1s peaks are presented in Table 3. The fitting components have been attributed as the following. On the carbon C1s peak: carbides (284.0 eV), C–C, C=C and C–H bonds (285.0 eV), C–O bonds (286.5 eV), C=O bonds (287.8 eV), O–C=O bonds (289.0 eV). On the oxygen O1s peak: UO_2, Fe_2O_3 and FeO (530.0 eV), O=C (532.0 eV), O–C (533.5 eV) [11]. The chemical forms of carbon (C–C, C–O, C=O, O–C=O) are characteristic of a contamination layer (0–3 nm). The chemical forms of oxygen show that a metallic oxide is present just under the contamination layer. A few percent of uranium carbide or iron carbide is also detected.

The chemical analysis results obtained by decomposition of $U4f_{7/2}$ and $Fe2p_{3/2}$ are presented in Table 4. The form of the U4f peak is complex (Fig. 5): $U4f_{7/2}$ and

Table 2
Elementary composition (at.%) of UFe_2 surface by XPS

Analysed thickness (nm)	θ (°)	% C	% O	% U	% Fe	U/Fe
0–7	0	22.54	55.04	10.20	12.22	0.835
0–3.5	60	44.80	45.00	7.37	2.83	2.605
0–2.5	70	49.25	41.65	7.13	1.97	3.620
0–2	75	49.05	41.20	7.73	2.02	3.825

Table 3
Chemical forms of carbon and oxygen in UFe_2 material by XPS as a function of θ

θ (°)	% carbide	% C–C	% C–O	% C=O	% O–C=O	% Metallic oxides	% O–C	% O=C
0	2.65	53.8	17.5	14.4	11.65	53.65	39.00	7.35
60	1.2	64.8	19.0	7.2	7.8	43.4	46.45	10.15
70	0.85	65.7	19.4	7.2	6.85	46.5	40.15	13.35
75	0.8	67.4	19.7	6.5	5.6	46.95	40.80	12.25

Table 4
Chemical forms of uranium and iron in UFe_2 material by XPS as a function of θ

θ (°)	% $U_xFe_yO_z$	% UO_2	% UO_{2+x}	% $Fe_xU_yO_z$	% Fe2+	% Fe3+
0	8.8	77.25	13.95	12.5	38.75	48.75
60	4.6	79.15	16.25	8.8	32.9	58.3
70	5.65	76.35	18.0	8.5	34.3	57.2
75	4.3	79.3	16.4	11.1	47.6	41.3

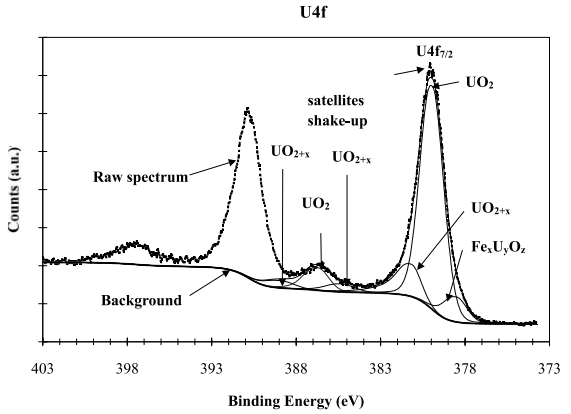

Fig. 5. XPS spectrum of U4f for UFe_2 compound oxidised at room temperature for 10 h.

$U4f_{5/2}$ are centred at 380 and 391 eV. A satellite shake-up at 7 eV of these two peaks and a secondary satellite shake-up at 9 eV (Fig. 5) are present. They are characteristic of two phases of uranium oxide: UO_2 (the main phase) and UO_{2+x}. The existence of a ternary oxide (confirmed by the ToF-SIMS analyses) is proved by the presence of a low energy (378.6 eV) peak which is clearly shifted up compared to U^0 (377.3 eV). The chemical analysis of iron shows that iron is mainly in Fe2+ (probably FeO) and Fe3+ chemical states. A low energy component is also found at 707 eV (Fig. 6); it should correspond to iron in the ternary oxide $U_xFe_yO_z$ evidenced by the decomposition of the $U4f_{7/2}$ peak. The fitting components have been attributed as following. On the uranium $U4f_{7/2}$ peak: $U_xFe_yO_z$ (378.6 eV), UO_2 (380.0 eV), UO_{2+x} (381.25 eV). On the iron $Fe2p_{3/2}$ peak: $Fe_xU_yO_z$ (707.0 eV), Fe2+ (709.5 eV), Fe3+ (711.0 eV) [10].

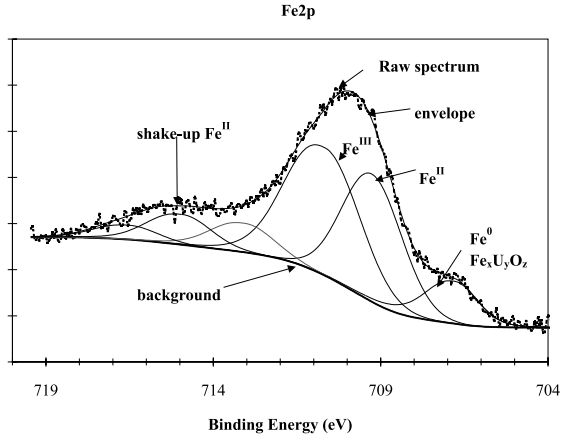

Fig. 6. XPS spectrum of $Fe2p_{3/2}$ for UFe_2 compound oxidised at roomtemperature for 10 h.

AES and SIMS with ion abrasion allow to study deeper than XPS the UFe_2 compounds. Several hundreds of nm in depth were measured by AES and SIMS analyses while the XPS depth analysis is lower than 10 nm. As clarified below, the AES and SIMS analyses show that the surface of UFe_2 oxidised for 45 h, 72 h, 17 days at 63°C and for 4 and 10 h at room temperature are constituted of a pile of layers of the same physical–chemical nature and composition (Fig. 7) because in each different layer, the secondary intensities of each ion species on the SIMS profile are of the same order (Fig. 8) and moreover, the AES concentrations are very similar (Fig. 9). The thickness of the layers varies as a function of the conditions of oxidation. The analyses are reproducible. The surface of UFe_2 is constituted of three overlayers covering UFe_2.

A high concentration of carbon is detected onto the surface by AES. As revealed by XPS, this indicates that the first overlayer is a carbon contamination layer of 2 nm (60% and 70% on the Fig. 9).

As determined by XPS with variable angle, the metallic oxide layer is composed of a mixture of UO_2 and UO_{2+x}, iron oxide and a ternary oxide $U_xFe_yO_z$. The physical–chemical nature of the major phases of layers 2 and 3 are the same because the secondary ion intensities of each species vary only of one order of magnitude in these two layers (Fig. 8).

The first nm of the metallic oxide layer (layer 2) is depleted in iron as observed by XPS with variable angle. The AES ratio Fe/U increases continuously from 1 to 2 onto 20 to 40 nm (from the first nm in the Figs. 9(b)–(d)). This indicates a segregation of uranium or iron. This iron depleted layer corresponds to a region where the secondary ion emissions decrease continuously by a factor 2 to 10 (the first 20 nm of the Figs. 8(b)–(d)). Moreover, the AES carbon concentration falls from 60% to zero in the 10 to 20 first nm (Fig. 9).

The metallic oxide layer (layer 3) has a constant concentration ($\Delta C/C <$ a few %). Since the variations of

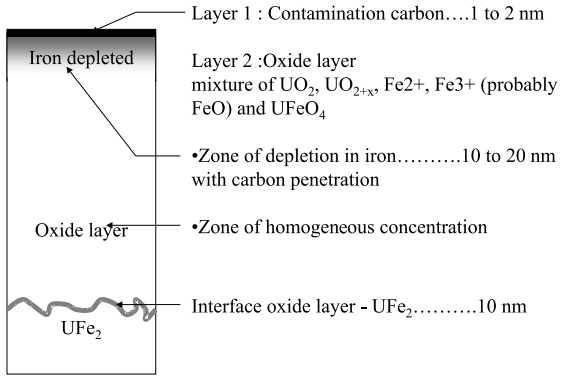

Fig. 7. Diagram of UFe_2 compound surface.

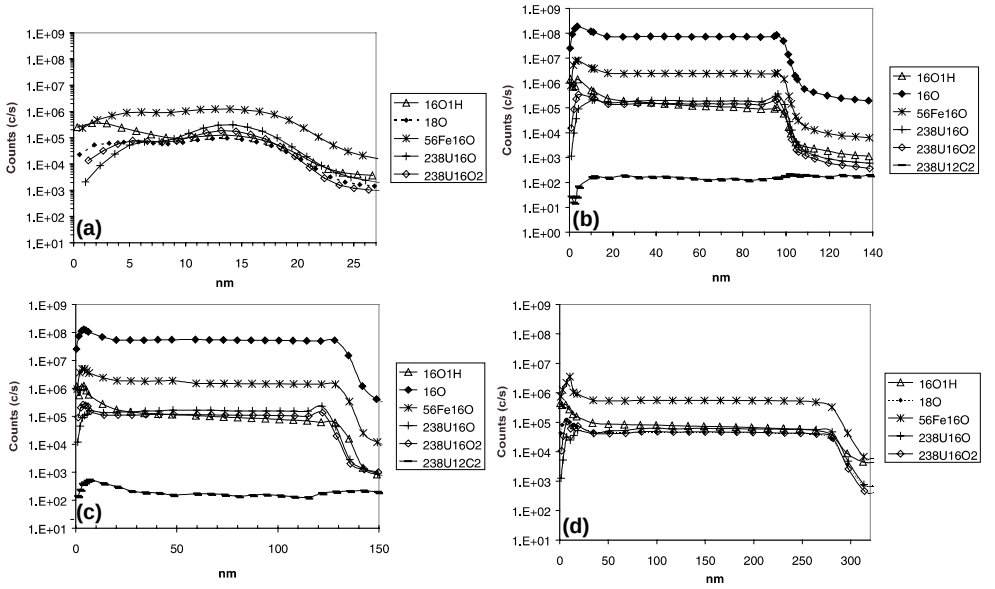

Fig. 8. SIMS profile of UFe_2 compound oxidised: (a) for 4 h at room temperature; (b) for 45 h at 63°C; (c) for 72 h at 63°C; (d) for 17 days at 63°C.

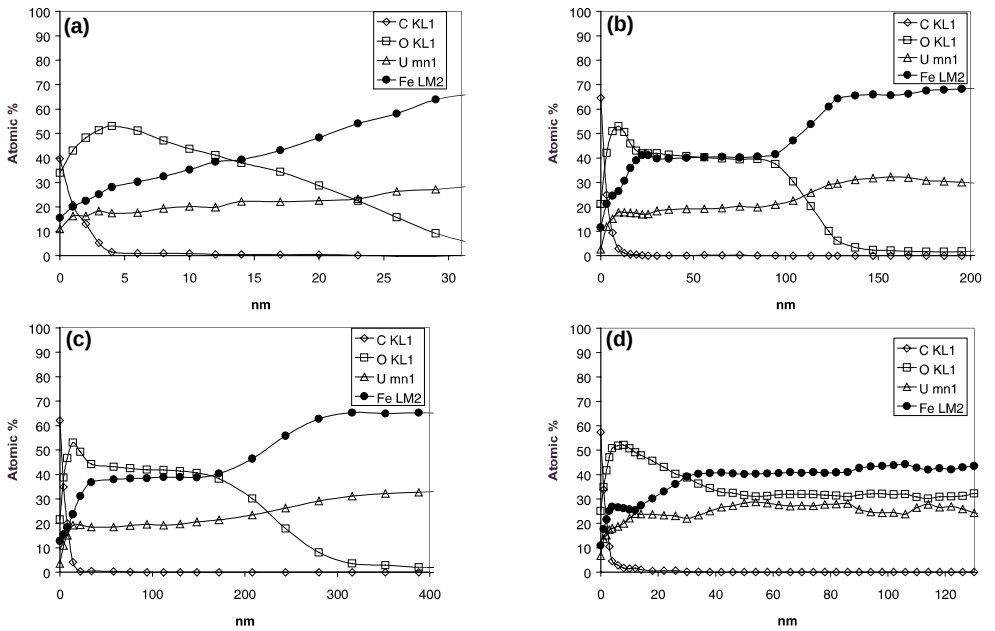

Fig. 9. Auger profile of UFe_2 compound oxidised: (a) for 4 h at room temperature; (b) for 45 h at 63°C; (c) for 72 h at 63°C; (d) for 17 days at 63°C.

the AES concentrations are weaker than the precision of the measurements, they are not characteristic of real variations of concentrations. Moreover, in this layer (from 17 to 90 nm on the Fig. 8(b)) the secondary ion intensities of $^{16}O^-$, $^{56}Fe^{16}O^-$, $^{238}U^{16}O^-$, $^{238}U^{12}C_2^-$ and $^{238}U^{16}O_2^-$ are constant (variation lower than a few percents) (Fig. 9). As a result, the concentration of this layer is constant ($\Delta C/C <$ a few percent). The secondary ion intensity of $^{16}O^1H^-$ decreases continuously (factor 10) over 80 nm even when the other ion intensities are constant. Assuming that the hydrogen concentration is proportional to the intensity of the ion $^{16}O^1H^-$ and that

the emission efficiency of $^{16}O^-$ and $^{16}O^1H^-$ are equal, the hydrogen concentration could be estimated (Fig. 8). The atomic concentration of hydrogen decreases quasi-linearly from 0.1% to 0.01% between the beginning and the end of this layer. The chemical form of hydrogen is probably OH^- [4].

The thickness of the oxide–UFe_2 interface is 10–100 nm, probably as the consequence of a rough interface due to ion abrasion.

Assuming that the ion emission efficiency of $^{16}O^-$ in the oxide layer and in UFe_2 is equal and proportional to the oxygen concentration, the bulk UFe_2 contains 0.1% of oxygen.

ToF-SIMS gives some supplementary information about the physical–chemical nature. Several hundreds of nm in depth were measured by ToF-SIMS analyses. ToF-SIMS analyses have been performed on UFe_2 oxidised for 8 h in air at room temperature (Fig. 10) with Cs primary ions. The detection of ternary ions ($UFeO_2$ and $UFeO_3$) and UO_x ions proves respectively the existence of a ternary oxide $UFeO_x$ and a uranium oxide UO_2 and/or UO_{2+x}. O^- and OH^- ions could result from U–O and Fe–O bonds. O_2^- ions are characteristic of oxygen in the O_2 form. The absence of Fe_2O_x fragment ions reveals the absence of Fe_2O_3 form. As a result, Fe3+ detected by XPS do not originate from Fe_2O_3. No U–U bonds are detected. The presence of UC and UC_2 ions reveals the presence of uranium-carbide. No ion characteristic of iron carbide is found. As a result, UFe_2 sample does not contain any iron carbides. Finally, the oxide layer is constituted of UO_{2+x}, FeO_x (probably FeO), a ternary oxide $UFeO_z$ (very probably $UFeO_4$ [13]) and a few percent of uranium carbide.

To resume these measurements:

- All the analysis techniques reveal a contamination carbon layer in the first nm.
- The oxide layer is constituted of a mixture of $UO_2, UO_{2+x}, UFeO_x$ (detected by ToF-SIMS and XPS with variable angle), of Fe2+ (probably FeO) and Fe3+. The first nm of the metallic oxide layer is depleted in iron onto several tenth nm. Further, the oxide layer concentration is constant. Fe3+ ions do not originate from Fe_2O_3 (ToF-SIMS result). The proportion of the different phases in the oxide layer has been estimated by using the following hypotheses:
  1. The ratio Fe/U is two (like UFe_2);
  2. The decomposition of iron and uranium peaks is that obtained with XPS at normal angle detection;
  3. The concentration of the ternary oxide is 8.8% of the uranium concentration;
  4. The components Fe2+ and Fe3+ are attributed to FeO.

With these hypotheses, the oxide layer is constituted by 34% of UO_2 and UO_{2+x}, 61.7% of FeO (26.1% of Fe2+ and 34.8% of Fe3+), 3.3% of $UFeO_4$ and 1–0% of uranium carbide.

Similarly, the initial stage of oxidation of a U–14.1% Nb has been studied. Oxidation by O_2 produces a thin oxide overlayer of stoichiometric UO_2 intermixed with Nb_2O_5 [14] and oxidation of a U–14.1% Nb by DO_2 induces a depletion of Nb in the outermost surface region and oxidation of uranium in the near surface [14].

The native oxidation of polycrystalline UFe_2 at room temperature has already been studied by exposition in CO and CO_2 [7,15]. The uranium is in the first time, oxidised in UO_2 and segregates to the surface. The complete oxidation of uranium is followed by the oxidation of iron and a segregation of iron towards the surface. The ratio Fe/U is nevertheless less than 2. The iron is a mixture of Fe2+ and Fe3+. Schultz et al. [15]

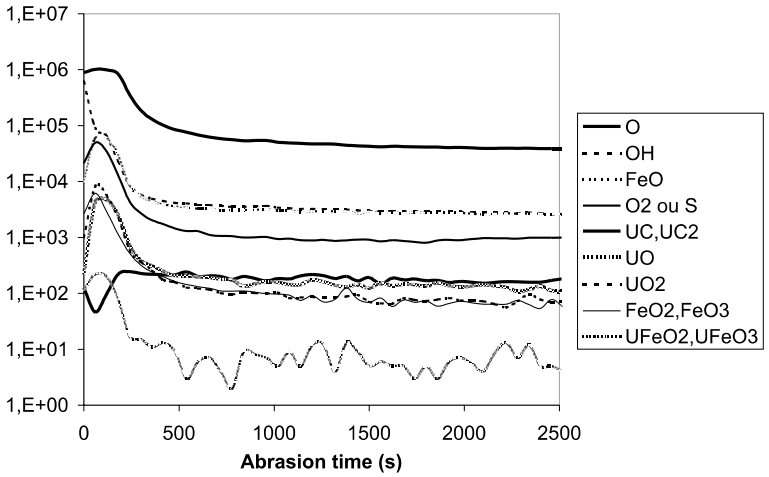

Fig. 10. ToF-SIMS profile of UFe_2 compounds for 10 h at room temperature.

Table 5
Thickness of the different overlayers found in the surface of UFe_2

Description	17 h 63°C (nm)	72 h 63°C (nm)	45 h 63°C (nm)	4 h at 10 h at Ta (nm)
Contamination carbon	$\leqslant 2$	$\leqslant 2$	$\leqslant 2$	$\leqslant 2$
Oxide layer depleted in iron	15	5–20	10-30	$\approx$2–10
Oxide layer (U, Fe, O)	300	110–210	80–120	$\approx$3–30
Metallic uranium	+	+	+	+

suggest that a mixed oxide ($U_xFe_yO_z$) is present. The reaction with CO and CO_2 is very similar to that of O_2 with nevertheless carbon penetration. The results of our study are in agreement with this work and prove the existence of a few percent of a mixed oxide $UFeO_4$ in the oxide layer.

An AES study of the oxidation behaviour in the intermetallic compound UFe_2 concludes that there is a large segregation of uranium at the surface as we found. Absorbed oxygen reacts only with the uranium and forms a stable oxide layer at the surface, which prevents further oxygen diffusing into the solid. As a result, the iron remains in the metallic form even after prolonged oxygen exposure [16]. As Schultz et al. [15], we observe an oxidation of iron (by XPS and ToF-SIMS). Nevertheless, the oxidation conditions are an air exposition in our study and not an exposition to O_2 alone.

An iron depletion is exhibited by AES, SIMS, and by XPS with variable angle in the first 5–20 nm, Iron or uranium segregates. This depletion has already been reported [7]. Moreover, Schultz et al. [7] have observed that ion bombardment produces a more important depletion in iron than a mechanical abrasion. XPS analysis with variable angle of detection is performed without any ion abrasion and an iron depletion is still observed. Thus iron depletion cannot be attributed to an ion bombardment. In this region, the AES concentration of carbon falls to zero. The carbon atoms diffuse (between 0 and 20 nm) and form a uranium carbide preferentially to an iron carbide (proved by this study by ToF-SIMS). Schultz et al. have also observed that carbon atoms penetrate into the sample, by complete dissociation of CO or CO_2 [7]. In the present study, carbon can originate from trace constituents of air (CO, CO_2).

Table 5 shows the different layers and their thickness as a function of oxidation times.

4. Conclusion

The oxidation of the uranium-materials due to air exposition at room temperature and 63°C is very similar and generates an important modification of surface. Moreover, the surface is covered by a layer of carbon contamination in its first nm. In uranium materials, the oxide layers are composed of compounds of UO_2 and UO_{2+x} with $0 < x < 0.25$. In UFe_2, the oxide layer is composed of a mixture of UO_2, UO_{2+x}, Fe2+ and Fe3+ (more probably FeO), 4% of a mixed oxide $UFeO_z$ (probably $UFeO_4$) and about 1% of uranium carbide. No Fe_2O_3 or iron carbides appear at the surface of UFe_2 (ToF-SIMS result). The proportion of each phase in the metallic oxide layer has been estimated from the normal angle XPS chemical analyses: 34% of UO_2–UO_{2+x}, 61.7% of FeO (26.1% of Fe2+ and 34.8% of Fe3+), 3.3% of $UFeO_4$ and 1–0% of uranium carbide. This oxide layer in UFe_2 is iron depleted over a thickness of 10 to 20 nm. Moreover, carbon diffuses in the first 20 nm of the material to form uranium carbide and no iron carbide.

This progress in the knowledge of the surface of uranium material will improve the accuracy of XPS. As an example, a good description of the surface structure associated with a multilayer software for WDS-EPMA will allow us to improve the accuracy of the bulk concentration by removing the surface contribution.

Acknowledgements

This work has been carried in the CEA. The authors wish to acknowledge M. Botreau, C. Berthier, C. Fucili and C. Fournier for their contributions.

References

[1] K.A. Winer, Dissertation, Abstracts Int. 46 (11B) (1985) 3975.
[2] S. Orman, G. Picton, J.C. Ruckman, Oxid. Met. 1 (2) (1969) 199.
[3] M.McD. Backer, L.N. Less, S. Orman, Trans. Faraday Soc. 62 (1966) 2513.
[4] K. Winer, C.A. Colmenares, R.L. Smith, F. Wooten, Surf. Sci. 183 (1987) 67.
[5] S. Orman, in: J.J. Shrier (Ed.), Oxidation of Uranium and Uranium Alloys in Physical Metallurgy of Uranium Alloys, Butterworths, London, 1976.
[6] W. McLean, C.A. Colmenares, R.L. Smith, G.A. Somorjai, Phys. Rev. B 25 (1) (1982) 8.
[7] J.C. Schultz, C.A. Colmenares, J. Naegle, J.C. Spielet, Surf. Sci. 198 (1988) 301.
[8] C. Merlet, in: E.S. Etz (Ed.), Proc. Microbeam Analysis, VCH, 1995, 203.

[9] M.P. Seah, W.A. Dench, Surf. Interface Anal. 1 (1979) 2.
[10] J.F Moulger, W.F. Stikle, P.E. Sobol, K.D. Bomden, in: Jill Chastain (Ed.), Handbook of X-ray Photoelectron Spectroscopy, Perkin Elmer, USA, 1992.
[11] T. Gouder, C. Colmenares, J.R. Naegele, J. Vertbist, Surf. Sci. 210 (1989) 280.
[12] C.A. Colmenares, in: G.M. Rosenblatt, W.L. Worrell (Eds.), Progress in Solid State Chemistry, vol. 15, Pergamon, New York, 1984, p. 257.
[13] M. Bacmann, E.F. Bertaut, Bull. Soc. Fr. Minéral. Cristallogr. (1967) 257.
[14] W.L. Manner, J.A. Lloyd, R.J. Hanrahan Jr., M.T. Paffett, Appl. Surf. Sci. 150 (1999) 73–88.
[15] J.C. Schultz, C.A. Colmenares, J. Nagele, J.C. Spirlet, Inorg. Chim. Acta 140 (1987) 37.
[16] M. Erbudak, F. Stucki, Phys. Rev. B 32 (4) (1985) 2667.